

Supporting Information for

Development of a Double-Stapled Peptide Stabilizing both α -Helix and β -Sheet Structures for Degrading Transcription Factor AR-V7

Bohan Ma, ‡^[a] Donghua Liu, ‡^[a] Mengjun Zheng,^[b] Zhe Wang,^[c] Dize Zhang,^[a] Yanlin Jian,^[a] Jian Ma,^[a] Yizeng Fan,^[a] Yule Chen,^[a] Yang Gao,^[a] Jing Liu,^[a] Xiang Li, *^[b] and Lei Li *^[a]

[a] Department of Urology, The First Affiliated Hospital, Xi'an Jiaotong University, Xi'an 710049, China

[b] School of Pharmacy, Second Military Medical University, 325 Guohe Road, Shanghai 200433, China

[c] Institute of Bioengineering, College of Chemical and Biological Engineering, Zhejiang University, Hangzhou, Zhejiang 310027, China

‡ These authors contributed equally to this work.

* Corresponding authors.

The corresponding authors' email addresses: Xiang Li: xiangli@smmu.edu.cn; Lei Li: lilydr@163.com.

KEYWORDS: double-stapled peptide; α -helix and β -sheet structures; PROTAC; AR-V7; prostate cancer.

Supplementary Figures

Figure S1

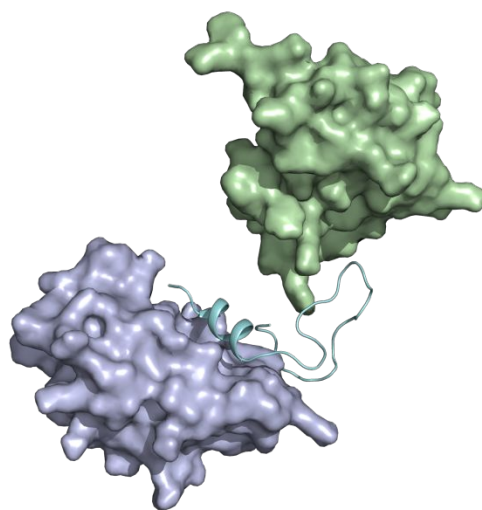


Figure S1. The structural modeling analysis of the complex between the linear peptide ARTC and MDM2 complexed with AR DNA binding domain.

Figure S2

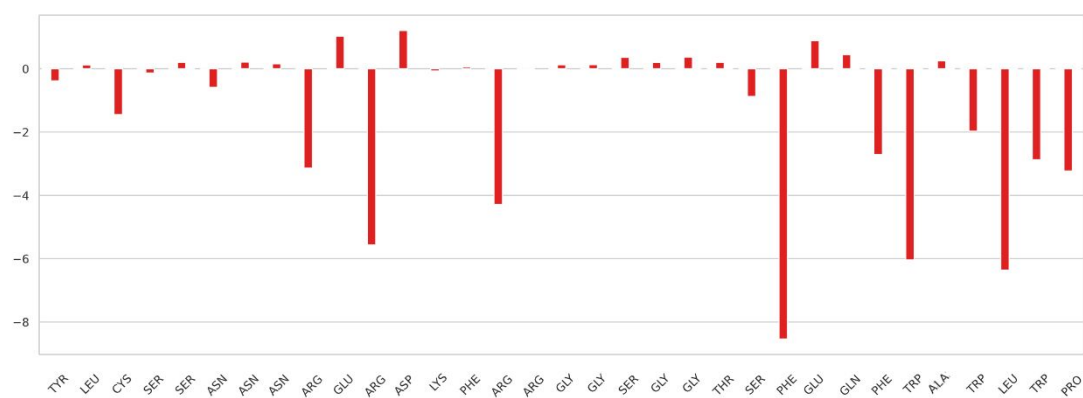


Figure S2. Amino acids at various locations were analyzed for their impact on binding to the androgen receptor DNA binding domain (AR DBD).

Figure S3

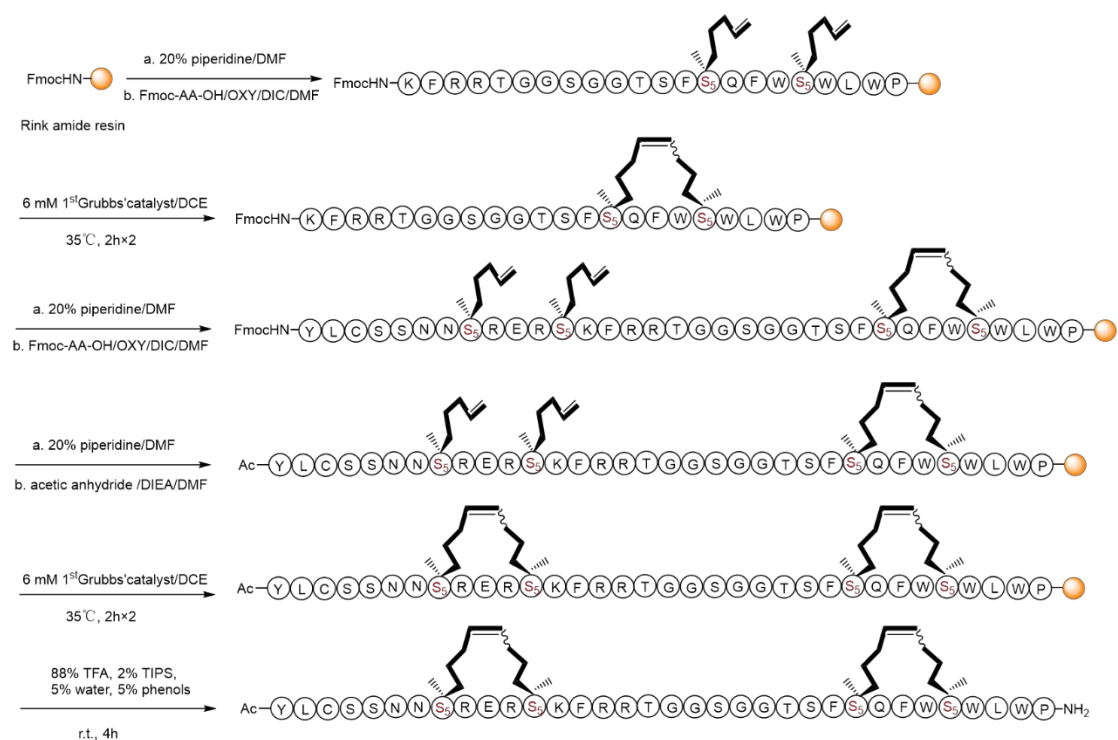


Figure S3. Synthetic route of double stapled peptides DSARTC.

Figure S4

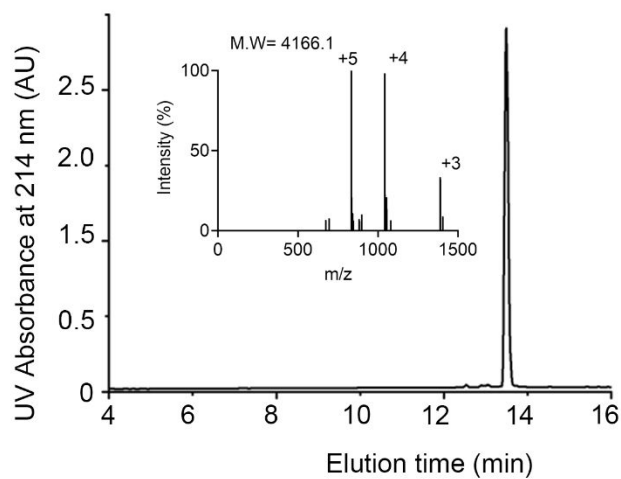


Figure S4. HPLC and MS characterization of DSARTC.

Figure S5

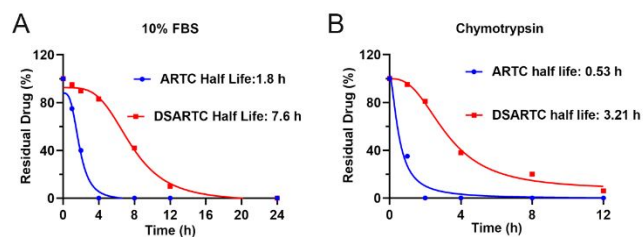


Figure S5. Stability detection of DSARTC. A) The serum resistance of the free peptide and DSARTC was tested in PBS containing 10% serum. B) The chymotrypsin resistance analysis of the free peptide and DSARTC.

Figure S6

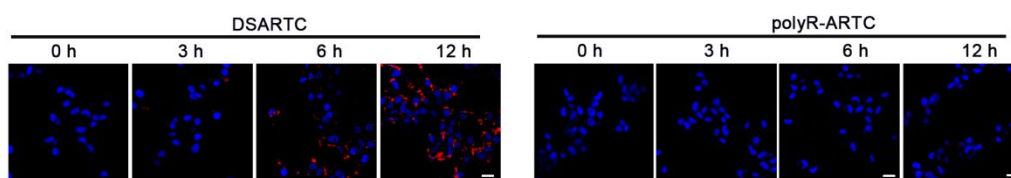


Figure S6. Cellular uptake analysis comparing DSARTC and polyR-DSARTC by confocal at a used concentration of 5 μ M in C4-2 cell lines.

Figure S7

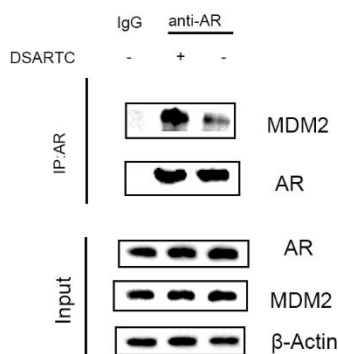


Figure S7. IB analysis of WCL and anti-AR immunoprecipitated (IP) from C4-2 cells with or without DSARTC treatment.

Figure S8

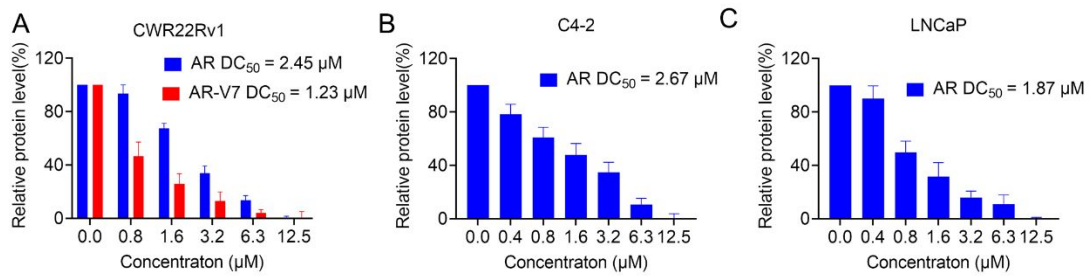


Figure S8. Statistical Analysis of the degradation ability of AR and AR-V7 by DSARTC.

Figure S9

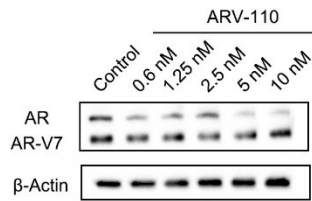


Figure S9. The degradation ability test of ARV110 for AR and AR - V7 on CWR22Rv1 cells.

Figure S10

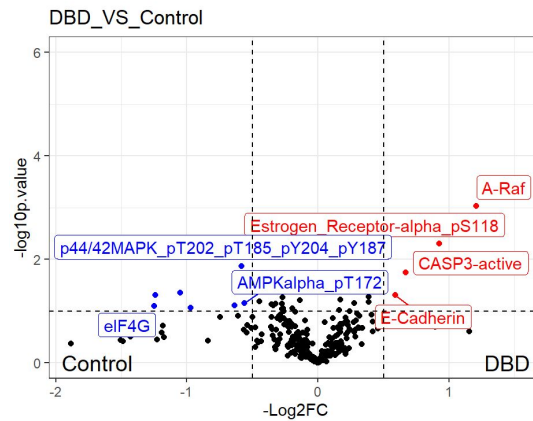


Figure S10. Volcano plots of protein analysis in CWR22Rv1 cells after treatment with DSARTC for 24 h.

Figure S11

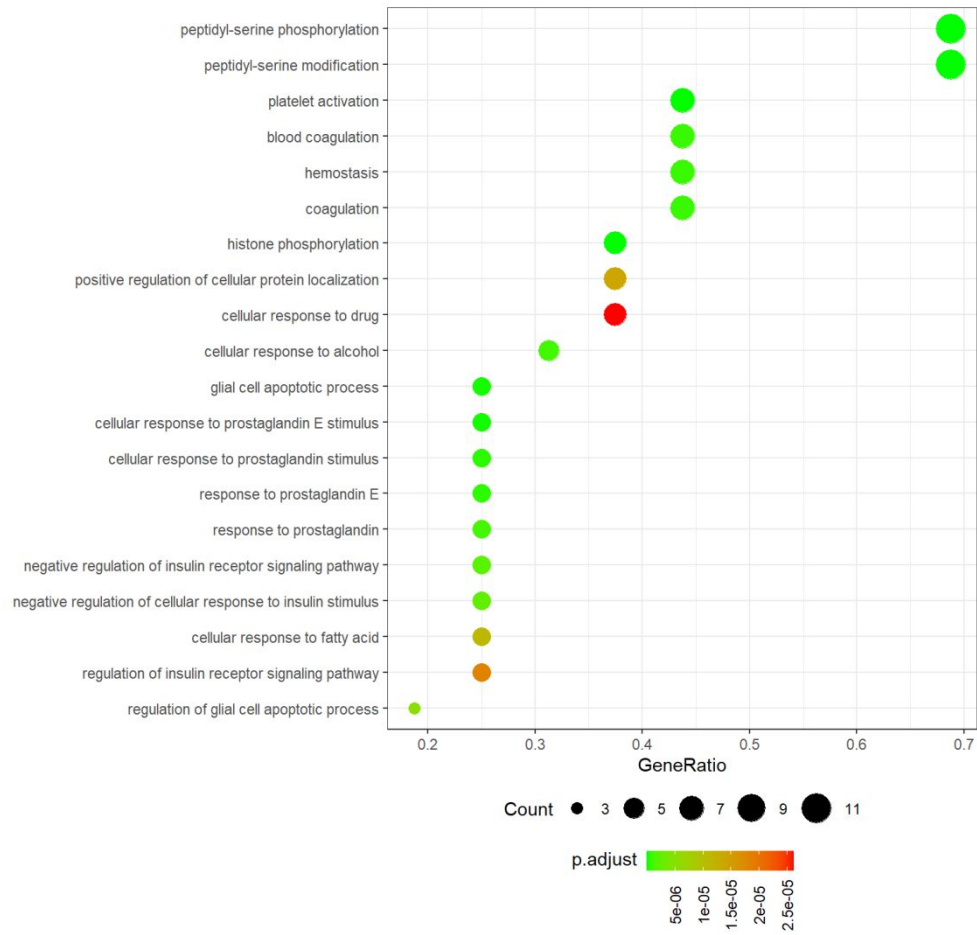


Figure S11. GO pathway enrichment analysis after DSARTC drug treatment compared to the control group in CWR22Rv1 cells.

Figure S12

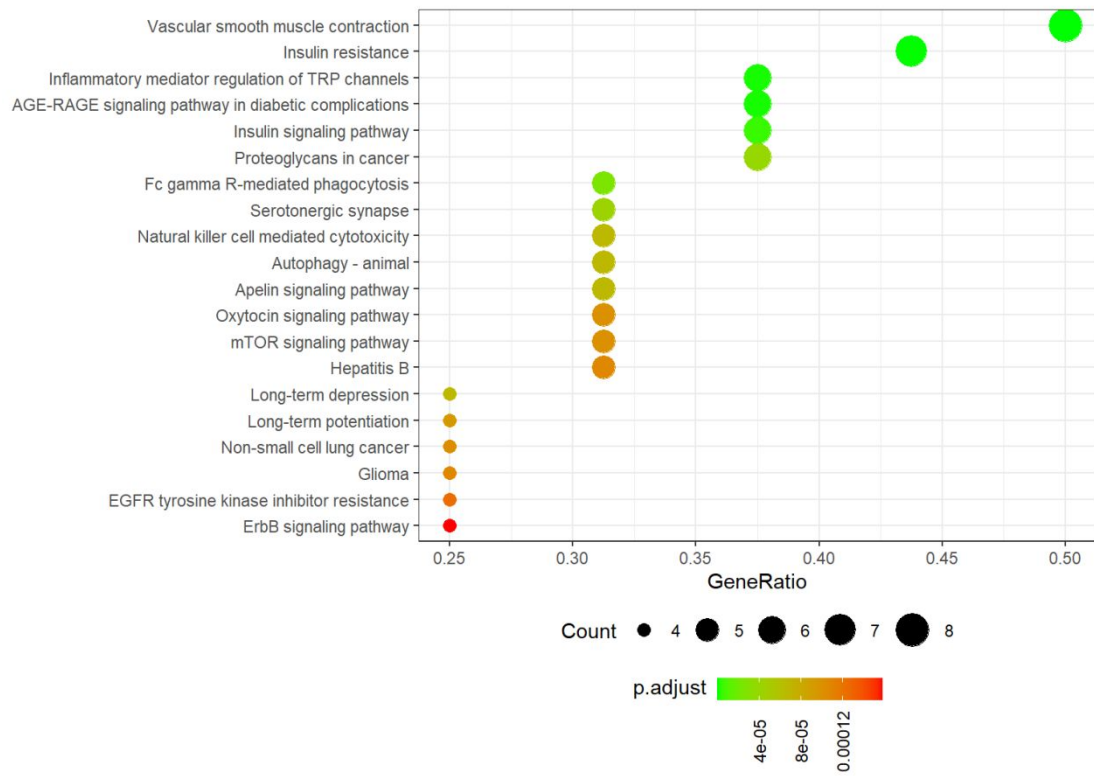


Figure S12. KEGG pathway enrichment analysis after DSARTC drug treatment in CWR22Rv1 cells.

Figure S13

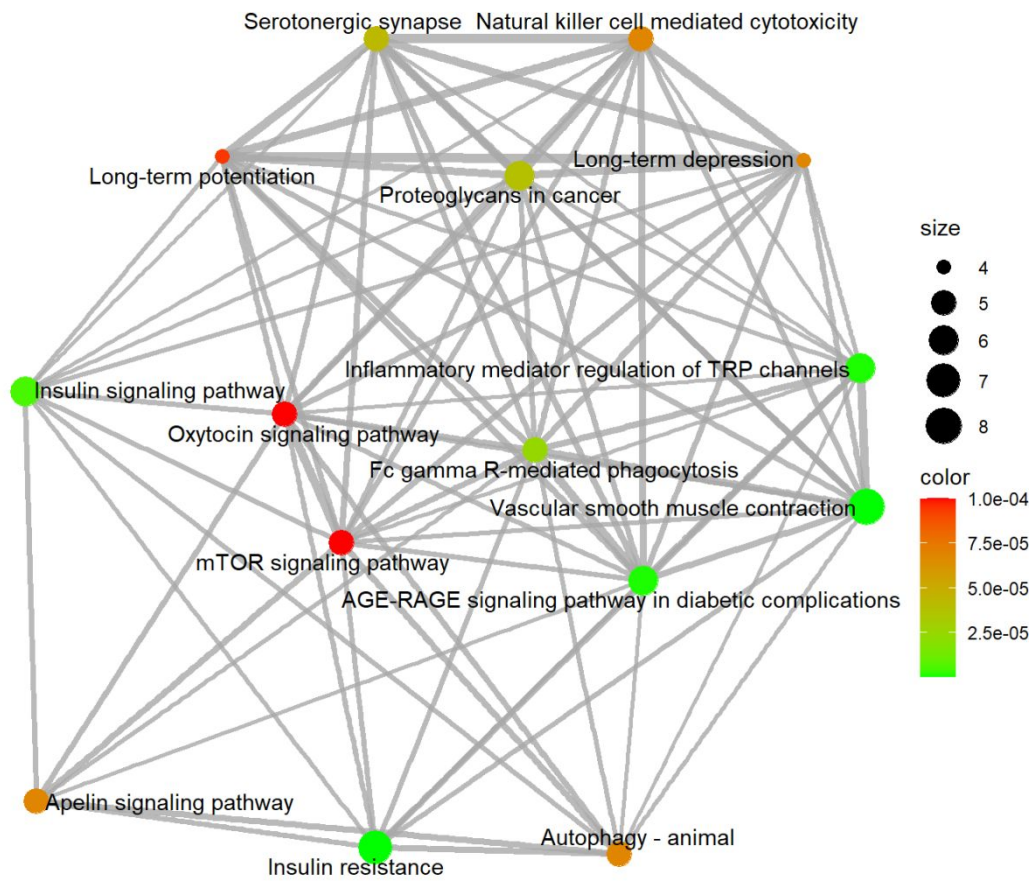


Figure S13. KEGG emapplot enrichment analysis after DSARTC drug treatment in CWR22Rv1 cells.

Figure S14

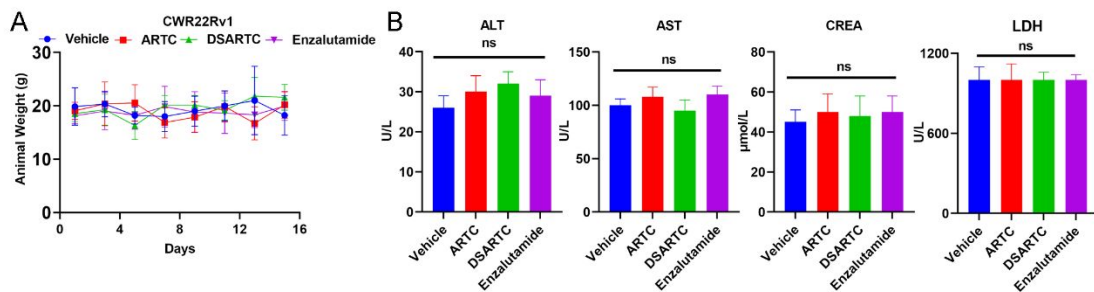


Figure S14. Safety analysis of DSARTC. A) Body weight change detection during drug treatment. B) Liver and kidney toxicity analysis after drug treatment.

